

Interaction between Heat Shock Proteins and Antimicrobial Peptides[†]

Laszlo Otvos, Jr.,^{*,‡} Insug O,[‡] Mark E. Rogers,[§] Patricia J. Consolvo,[‡] Barry A. Condie,[‡] Sandor Lovas,^{||} Philippe Bulet,[⊥] and Magdalena Blaszczuk-Thurin[‡]

The Wistar Institute, 3601 Spruce Street, Philadelphia, Pennsylvania 19104, M-Scan, Inc., 606 Brandywine Parkway, West Chester, Pennsylvania 19380, Department of Biomedical Sciences, Creighton University, 2500 California Street, Omaha, Nebraska 68178, and Institute de Biologie Moleculaire et Cellulaire, 15 Rue Rene Descartes, 67084 Strasbourg, Cedex, France

Received June 5, 2000; Revised Manuscript Received September 20, 2000

ABSTRACT: Drosocin, pyrrhocoricin, and apidaecin, representing the short (18–20 amino acid residues) proline-rich antibacterial peptide family, originally isolated from insects, were shown to act on a target bacterial protein in a stereospecific manner. Native pyrrhocoricin and one of its analogues designed for this purpose protect mice from bacterial challenge and, therefore, may represent alternatives to existing antimicrobial drugs. Furthermore, this mode of action can be a basis for the design of a completely novel set of antibacterial compounds, peptidic or peptidomimetic, if the interacting bacterial biopolymers are known. Recently, apidaecin was shown to enter *Escherichia coli* and subsequently kill bacteria through sequential interactions with diverse target macromolecules. In this paper report, we used biotin- and fluorescein-labeled pyrrhocoricin, drosocin, and apidaecin analogues to identify biopolymers that bind to these peptides and are potentially involved in the above-mentioned multistep killing process. Through use of a biotin-labeled pyrrhocoricin analogue, we isolated two interacting proteins from *E. coli*. According to mass spectrometry, Western blot, and fluorescence polarization, the short, proline-rich peptides bound to DnaK, the 70-kDa bacterial heat shock protein, both in solution and on the solid-phase. GroEL, the 60-kDa chaperonin, also bound in solution. Control experiments with an unrelated labeled peptide showed that while binding to DnaK was specific for the antibacterial peptides, binding to GroEL was not specific for these insect sequences. The killing of bacteria and DnaK binding are related events, as an inactive pyrrhocoricin analogue made of *all-D*-amino acids failed to bind. The pharmaceutical potential of the insect antibacterial peptides is underscored by the fact that pyrrhocoricin did not bind to Hsp70, the human equivalent of DnaK. Competition assay with unlabeled pyrrhocoricin indicated differences in GroEL and DnaK binding and a probable two-site interaction with DnaK. In addition, all three antibacterial peptides strongly interacted with two bacterial lipopolysaccharide (LPS) preparations in solution, indicating that the initial step of the bacterial killing cascade proceeds through LPS-mediated cell entry.

One of the most serious emerging health concerns today is the appearance and spread of antibiotic-resistant bacterial strains (1). It is thus becoming increasingly important to identify antimicrobial compounds with novel modes of action for which the bacteria are unable to mount a quick response and to build resistance. Perhaps the most promising among these novel compounds is a family of antibacterial peptides originally isolated from insects (2–6). Table 1 lists the related peptide sequences. Some of these were shown to act in a stereospecific manner on a target bacterial protein (4, 7, 8). In contrast, studies on model membranes as well as on live bacteria have indicated that other types of antibacterial peptides provoke an increase in plasma membrane permeability (9). A direct correlation between antibiotic effect and membrane disruption has been found for defensins from mammals and insects, magainins, and cecropins (10–13).

Table 1: Comparison of Sequences from Drosocin (*Drosophila melanogaster*) Formaein 1 (*Myrmecia gulosa*), Pyrrhocoricin (*Pyrrhocoris apterus*), N-Terminal Region of Dipterocin (*Phormia terranova*), and Apidaecin 1A (*Apis mellifera*)^a

drosocin	G K P R P Y S P R P T S H P R P I R V
formaein 1	G R P N P V N N K P T P Y P H L
pyrrhocoricin	V D K G S Y L P R P T P P R P I Y N R N
dipterocin	D E K P K L I L P T P A P P N L P Q...
apidaecin 1a	G N N R P V Y I P Q R P R P H P R I

^a Threonine residues, glycosylated in the native peptides, are underlined.

However, such antibacterial peptides that lyse bacterial membranes are potentially toxic to eucaryotic cells and are, therefore, unsuitable as a systemic drug. This highlights the potential of drosocin, apidaecin, and pyrrhocoricin. None of these peptides lyse sheep erythrocytes, and in addition, pyrrhocoricin also appears to be completely nontoxic to COS cells of primate origin (14). Significantly, pyrrhocoricin and one of its analogues, Chex-pyrrhocoricin-Dap(Ac) designed to withstand protease cleavage, remain nontoxic in vivo and protect mice from live *Escherichia coli* challenge (14). Ideally, one hopes to identify a protein present only in

[†] This work is supported by NIH Grant GM45011.

^{*} To whom correspondence should be addressed. Telephone: 215-898-3772. Fax: 215-898-5821. E-mail: Otvos@wistar.upenn.edu.

[‡] Wistar Institute.

[§] M-Scan Inc.

^{||} Creighton University.

[⊥] Institute de Biologie Moleculaire et Cellulaire.

bacteria that carries a significant function. This target may form the basis of rational drug design efforts, as was first suggested for apidaecin (15).

Some antibacterial peptides are known to act as inhibitors of enzymes produced by the bacteria either by serving as a pseudo-substrate or by tight binding to the active site eliminating the accessibility of the native substrate (9). For example, histatins are capable of inhibiting a trypsin-like proteinase from *Bacterioides gingivalis* with an IC_{50} in the submicromolar range (16). Microbial serine protease(s) are also inhibited by the equine version of the peptide NAP-2 (17). Other peptides can control yet additional proteinases involved in inflammatory processes, such as the inhibition of furin by histatin 5 (18). There are significant similarities in the mechanism of action between the latter case and the pyrrocoricin-drosocin-apidaecin family. The bioactive secondary structure of drosocin has been suggested to comprise of two reverse turns, one at each terminal region, which constitute the binding sites to the target molecule (19). The general fold of native pyrrocoricin, as determined by nuclear magnetic resonance spectroscopy (NMR)¹ and circular dichroism spectroscopy, is similar (14). Also for pyrrocoricin, reverse turns are identified as pharmacologically important elements at the termini, bridged by an extended peptide domain (14). The recognition mechanism of histatin 5 involves a well-defined bioactive conformation of this 24-mer peptide, as was demonstrated by its selectivity to other proprotein convertases. In addition, the *all-D*-peptide remained inactive (18), just like for drosocin, pyrrocoricin, and apidaecin (7, 14, 15).

As for apidaecin, recent results upheld the model of permease/transporter-mediated peptide uptake in bacterial cells (20). The proposed mechanism involves an initial, nonspecific encounter of the peptide with an outer membrane component, followed by invasion of the periplasmic space and by a specific and essentially irreversible engagement with a receptor/docking molecule that may be inner membrane-bound or otherwise associated, most likely a component of a permease-type transporter system. In the final step, the peptide is translocated into the interior of the cell where it meets its ultimate target, perhaps one or more components of the protein synthesis machinery (20).

In this paper, we identified some interacting macromolecular targets of this cascade to provide biopolymers on which the drug design process can proceed. We used a combination of immunoaffinity purification, mass spectrometry (MS), and a series of biochemical assays to show that pyrrocoricin, drosocin, and apidaecin specifically bind to the bacterial heat shock protein DnaK but not to the appropriate human equivalent. An inactive pyrrocoricin variant and a control, unrelated peptide did not bind. The insect antibacterial peptides also interacted with the LPS of Gram-negative bacteria and GroEL, the bacterial chaperonine. However, the interaction with GroEL did not seem to be specific for these peptide sequences.

MATERIALS AND METHODS

Immunoaffinity Purification of the Target Proteins. (a) French-pressed bacterial cell lysate (50 mL) was centrifuged at 2500 rpm for 20 min to remove residual cells and cell wall. (b) A total of 4.5 mL of bacterial supernatant (*E. coli* strain TG-1) was mixed with 150 μ g of biotin-K-pyrrocoricin peptide diluted in 1 mL of phosphate-buffered saline (PBS), and the mixture was incubated at room temperature for 3 h followed by centrifugation at 2000 rpm for 20 min. (c) A total of 1.5 mg of anti-biotin monoclonal antibody (clone BN34) coupled to agarose was washed with PBS to remove NaN_3 , and the peptide-lysate mixture was loaded onto the column (1.5 mL). The column was extensively washed with PBS. (d) The target proteins were eluted with 5 column vol of 0.1 M glycine (pH 2.9), and the eluant was immediately neutralized with 100 μ L of 1 M Tris-HCl (pH 8.0). Fractions of 1 mL were collected, and the fractions were analyzed for the presence of pyrrocoricin-binding proteins by 12% sodium dodecyl sulfate-polyacrylamide gel electrophoresis (SDS-PAGE) and a modified Western blot (peptide blot).

The Western-Blot Was Performed as Follows. (a) An aliquot of each fraction from the immunoaffinity column at 1:1 ratio was mixed with 50 μ L of Laemmli sample buffer (Bio-Rad), 5% of 2-mercaptoethanol was added, and the mixture was boiled for 3 min. A total of 10 μ L of the boiled samples was processed using 12% SDS-PAGE at 100 V for 1.5 h at room temperature. (b) The proteins from the gel were transferred to a nitrocellulose membrane (for the Western blot) or to poly(vinylidene difluoride) (PVDF) membrane (for staining with amidoblack), which were equilibrated with 25 mM Tris and 192 mM glycine buffer containing 20% methanol at 100 V for 2 h at 4 °C. The membrane was blocked with 5% milk in a PBS-0.05% Tween 20 buffer (PBST) overnight at 4 °C. (c) The membrane was incubated with 10 mL of 25 μ g/mL biotin-K-pyrrocoricin dissolved in PBST containing 1% bovine serum albumin (BSA) at room temperature for 1 h. After incubation, the membrane was extensively washed with PBST. (d) Streptavidin conjugated to horseradish peroxidase (Gibco-BRL) dissolved in 1% BSA-PBST was added to the membrane and was incubated with it at room temperature for 45 min. After being extensive washed with PBST, the membrane was treated with a chemiluminescence reagent, luminol-oxidizer (NEN), for 1 min. The membrane was exposed to a X-Omat blue XB-1 film (Kodak), and the film was developed.

***E. coli* Expressed Proteins.** Heat shock proteins and Ras, expressed or overexpressed in *E. coli*, were purchased from Sigma (St. Louis, MO), StressGen (Victoria, Canada), and Accurate (Westbury, NY). The purity of DnaK varied from 70% (StressGen) to 90% (Accurate). In addition to this uncertainty, Sigma has discontinued selling this item.

Mass Spectroscopy. Positive ion electrospray ionization-mass spectrometry (ESI-MS) was performed using a QToF instrument (Micromass, Manchester, U.K.). Samples were introduced via a nanospray source and needle in a solution of 50% aqueous acetonitrile. Daughter ion spectra were generated from the appropriate doubly charged parent ions using argon as the collision gas.

¹ Abbreviations: NMR, nuclear magnetic resonance spectroscopy; MS, mass spectrometry; PBS, phosphate-buffered saline; SDS-PAGE, sodium dodecyl sulfate-polyacrylamide gel electrophoresis; PBST, phosphate-buffered saline-Tween 20 buffer; BSA, bovine serum albumin; PVDF, poly(vinylidene difluoride); nano-ES, nano-electron-spray; LPS, lipopolysaccharide.

Fluorescence Polarization. The heat shock proteins were aliquoted in 4 and 2 μ M concentrations into borosilicate tubes in 100 μ L of final volume. 5(6)-Carboxyfluorescein-labeled peptides were added in 1 nM final concentration, and the tubes were incubated at 25 °C for 10 min. The extent of fluorescence anisotropy was measured on a Beacon 2000 fluorescence polarization instrument (PanVera) and was calculated as millipolarization values. The filters used were 485 nm excitation and 535 nm emission with 3 nm bandwidth.

Antibacterial Efficacy Assay. Antibacterial assays were performed in sterile 96-well plates (Nunc F96 microtiter plates) with a final volume of 100 μ L as described earlier (7). Briefly, 90 μ L of a suspension of a midlogarithmic phase bacterial culture at an initial 600 nm UV absorbance of 0.001 in poor broth medium was added to 10 μ L of serially diluted peptides in sterilized water. The final peptide concentrations ranged between 0.3 and 40 μ M. Plates were incubated at 30 °C for 24 h with gentle shaking, and growth inhibition was measured by recording the increase of the UV absorbance at 600 nm on a SLT Labinstruments 400 ATC microplate reader.

RESULTS

Earlier, we showed that biotin-K-pyrrocoricin kills *E. coli* D22 and TG-1 with IC₅₀ values of 100 nM and 10 μ M, respectively (14). On the basis of this observation, we hypothesized that the target protein from an *E. coli* lysate can be isolated by using the labeled peptide and that the complex can be purified through the attached biotin. In line with the weakest activity figure, we used the biotin-K-pyrrocoricin peptide at a concentration of 10 μ M during both purification of the interacting proteins and Western blotting. Pyrrocoricin-binding proteins were detached from the immobilized anti-biotin antibody in an acidic buffer, and the resulting peptide-target mixture was submitted to SDS-PAGE, followed by sequencing by MS. The fractions from the immunoaffinity purification showed proteins binding to biotin-K-pyrrocoricin in diverse amounts and purities. While the cleanest fractions containing proteins identifiable by pyrrocoricin binding on a modified Western blot (peptide blot) did not seem to contain sufficient protein for sequencing, the earliest eluting fraction, which contained a number of other proteins in lower quantities, had two principal proteinaceous components that were apparently suitable for MS. These two proteins exhibited molecular weights around 60–70 kDa (lane 10 in Figure 1A) when transferred to PVDF membrane and stained with 0.1% amidoblack 10B. The staining intensity of these bands was significantly increased after immunoaffinity purification as compared to untreated *E. coli* lysate. Figure 1B shows that the biotin-K-pyrrocoricin peptide labeled the 60–70-kDa bands strongly on Western blot. Two additional bands, one running with the front and another running close to the 15-kDa molecular weight marker, were also labeled with the peptide. The former band may represent the labeled peptide itself, which was also eluted from the immunoaffinity column. According to the amidoblack-stained gel, the 15-kDa band did not represent proteinaceous material at a level above the other contaminating proteins. We did not observe any alteration in the Western blot when live *E. coli* cells were treated with the biotin-labeled peptide and were subsequently lysed by

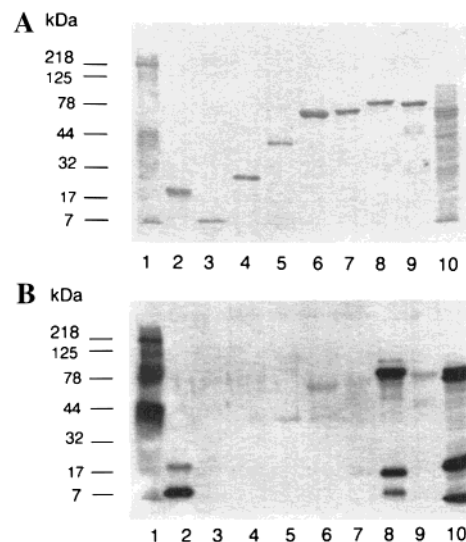


FIGURE 1: (A) SDS-PAGE of heat shock proteins and standards (2.8 μ g each). The lane assignments are as follows: 1, molecular weight markers; 2, Ras (Sigma); 3, GroES (Sigma); 4, GrpE (StressGen); 5, DnaJ (StressGen); 6, GroEL (Sigma); 7, Hsp60 (Sigma); 8, DnaK (Sigma); 9, Hsp70 (Sigma); and 10, the earliest eluting fraction from the immunoaffinity column. (B) Same protein preparations developed with biotin-K-pyrrocoricin. DnaK preparations purchased from StressGen and Accurate exhibited a pyrrocoricin-binding pattern similar to Sigma DnaK.

sonication indicating that the peptide efficiently entered into the cytoplasmic space.

The eluted fractions were submitted to another round of SDS-PAGE analysis that was designed to yield protein preparations suitable for subsequent sequencing. To this end, the gel containing the first fraction of the immunoaffinity column was stained using colloidal Coomassie Blue. A few very faint bands were stained in the 16–50-kDa range, apparently not suitable for sequencing. However, the two 60–70-kDa bands were clearly visible, even after some dilution of the sample. These bands were collectively excised from the gel together with a blank portion of the gel and subjected to in-gel tryptic digestion. The resulting peptides were extracted from the gel and purified using a reversed-phase cartridge. The peptide containing fractions were collected and analyzed by nano-ES mass spectrometry, which resulted in four doubly charged signals, potentially corresponding to tryptic fragments of *E. coli* proteins. These were at 922.5 [M + 2H]²⁺, 890.5 [M + 2H]²⁺, 799.3 [M + 2H]²⁺, and 1220.6 [M + 2H]²⁺, representing fragments Asp328-Arg345 (peptide 1) and Phe204-Phe219 (peptide 2) of GroEL as well as Ser453-Arg467 (peptide 3) and Val322-Arg345 (peptide 4) of DnaK, respectively. These peaks were submitted to MS-MS sequencing. Figure 2 demonstrates the daughter ions that could be assigned based on the fragmentation pattern of the tryptic peptides.

In the next step, we investigated whether commercially available eucaryotic and procaryotic heat shock proteins bind to the biotin-K-pyrrocoricin peptide in identical Western blotting conditions. We selected the bacterial chaperonins GroEL (60 kDa) and GroES (15 kDa) and three heat shock proteins, DnaK (70 kDa), DnaJ (40 kDa), and GrpE (25 kDa). These are involved in protein folding during the travel of nascent proteins from the ribosomes to GroEL (21–23). In addition, we included two mammalian heat shock proteins, Hsp60 (the human equivalent of GroEL) and Hsp70 (the

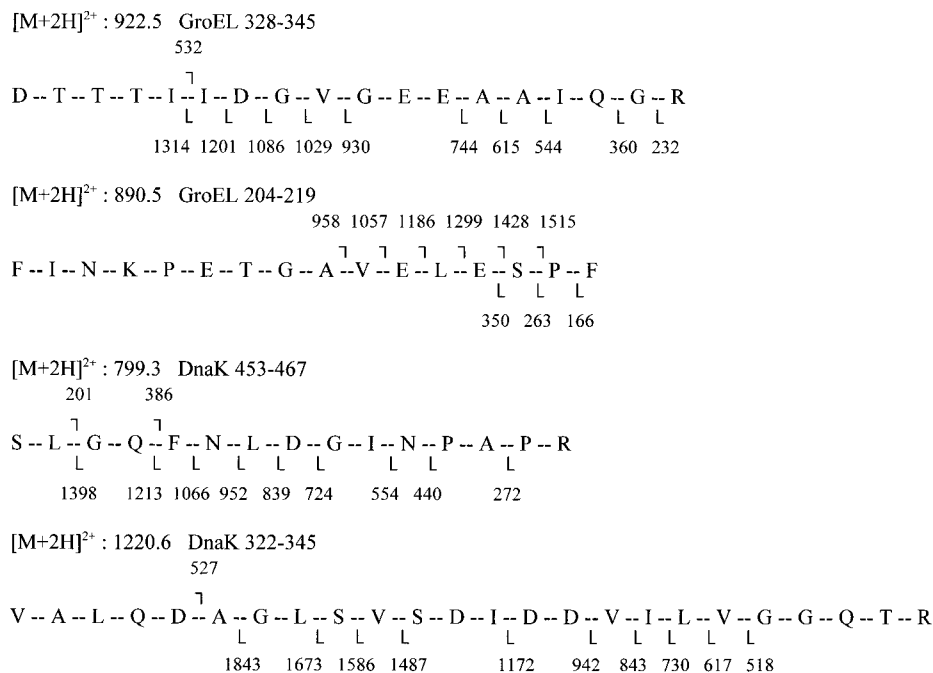


FIGURE 2: Daughter ions of tryptic peptide fragments 1–4 that could be assigned based on the fragmentation pattern of the nano-electrospray ionization tandem mass spectra. The fragmentation pattern verified the identity of the peptide sequences that were obtained from the database based on the masses of the doubly charged full fragments.

human equivalent of DnaK), to gain insight on why pyrrocoricin kills bacteria but is not toxic to mammalian cells and healthy mice. All these proteins were expressed or overexpressed in *E. coli*. As a negative control protein, we used the guanyl-nucleotide binding protein Ras (21 kDa), also expressed in *E. coli*. Approximately 2.8 μg of these proteins was loaded onto 12% SDS-PAGE, and the PVDF membrane was stained with amidoblack. The test proteins showed single bands in the expected molecular weight range with approximately equal intensities (Figure 1A). When tested for peptide binding, of the bands that could be stained with amidoblack, only the bacterial heat shock protein DnaK bound to biotin-K-pyrrocoricin (Figure 1B). The DnaK preparation had two additional non-proteinaceous bands that bound to the labeled pyrrocoricin, and the Ras preparation also had a non-proteinaceous peptide binding band. To make sure that we did not miss any peptide binding band, the gels depicted in Figure 1 were deliberately overloaded with both the fraction from the immunoaffinity purification and the test proteins. The nonspecific background level of binding is represented by the weak staining of the Ras protein band at 21 kDa. An additional above-background peptide-binding band was observed in the immunoaffinity purified fraction, running very close to DnaK. We ran a control peptide blot in which an unrelated biotin-labeled peptide, biotin-GPKG- β -tubulin 434–445 (24), was used as the “primary antibody”. This peptide was selected to serve as a negative control because it is highly negatively charged and does not share any sequence homology to the insect antibacterial peptides. In this blot, the very low molecular weight bands were stained from the eluted fraction and the DnaK preparation together with a near-DnaK-band from the early fraction (data not shown). A low molecular weight band from the Ras preparation, running with the front, was also stained. All these bands represented unspecific binding. From these studies, we confirmed that DnaK strongly bound to pyrrocoricin and concluded that the peptide also bound an

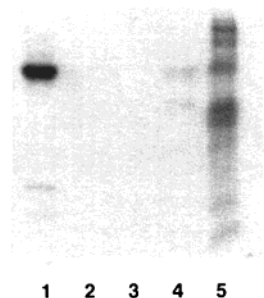


FIGURE 3: Western blot of LPS and control protein preparations. Approximately 1 μ g amounts of the proteins and LPS were loaded, and the blot was developed with biotin-K-pyrrhocoricin. Lane assignments: 1, DnaK; 2, *S. typhimurium* LPS; 3, *E. coli* LPS; 4, Hsp70 (all preparations from Sigma); 5, molecular weight markers.

unidentified component running at 15–20 kDa. Significantly, the peptide failed to bind Hsp70, the human equivalent of *E. coli* DnaK, over the background level.

Many cationic antibacterial peptides bind the negatively charged lipopolysaccharide (LPS) of Gram-negative bacteria (25). This suggested that the non-proteinaceous pyrrhocoricin-binding band might be bacterial LPS. This notion was further supported by the electrophoretic mobility pattern of *E. coli* LPS, which exhibits two stronger bands at low molecular weight regions and a smear of higher molecular weight bands (26). Because LPS isolated from various bacterial strains are readily available commercially, we purchased *E. coli* LPS as well as LPS from *Salmonella typhimurium* and tested their binding to biotin-K-pyrrhocoricin on Western blot. During the experimental conditions used, the peptide did not label LPS bands when these were nitrocellulose membrane-bound (Figure 3). The positive control DnaK was strongly labeled.

After learning that the antibacterial peptides interact with DnaK, we correlated the antimicrobial activity and DnaK binding. While native pyrrhocoricin made from *all*-L-amino

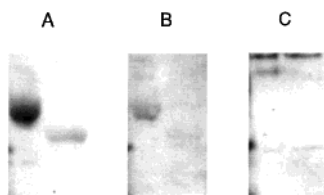


FIGURE 4: Binding of 1 μ g DnaK (Accurate) and GroEL (Stress-Gen) to biotin-K-pyrrolicorin made of L-amino acids (A), biotin-K-*all*-D-pyrrolicorin (B), and the negative control biotin-GPKG- β -tubulin 434–445 peptide (C). The left lanes in each panel contain DnaK; the right lanes contain GroEL. Blots B and C were developed with increased exposition times (to detect any band) as is indicated by the increased level of binding of the high molecular weight contaminating proteins.

acids kills *E. coli* D22 in nanomolar concentrations, a pyrrolicorin analogue made of *all*-D-amino acids is completely inactive (14). One microgram amounts of DnaK and GroEL proteins were tested for their binding to biotin-K-pyrrolicorin, biotin-K-*all*-D-pyrrolicorin, and biotin-GPKG- β -tubulin 434–445 on the peptide blot. As Figure 4 shows, while the L-peptide bound strongly to DnaK, the *all*-D-peptide bound only very weakly. The tubulin peptide did not bind at all. These experiments confirmed that killing of bacteria and DnaK binding are positively related events.

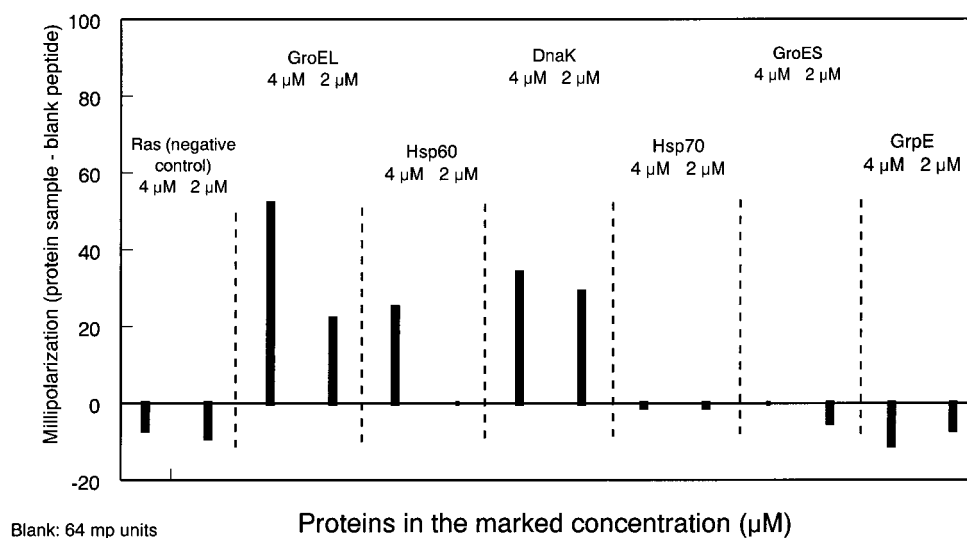
In the next step, we studied the binding of labeled variants of the short, proline-rich antibacterial peptides to the heat shock/chaperonin proteins and to LPS by fluorescence polarization, which technique is performed fully in solution. To this end, we synthesized four fluorescein-labeled peptides, fluorescein-K-pyrrolicorin, fluorescein-K-drosocin, fluorescein-K-apidaecin, and pyrrolicorin-K(fluorescein). The C-terminally labeled peptide was made to investigate the possibility of spatial separation of the active sites. From our earlier experiments, we know that pyrrolicorin and drosocin bind to the receptor(s) with their two terminal domains (14, 19). During fluorescence polarization, positive signals are detected only when the free rotation of the fluorescein attached to one of the interacting partners is slowed due to binding to the other partner when this label is not exceedingly far from the site of interaction. We also know that fluorescein-K-pyrrolicorin kills *E. coli* strains (with an IC_{50} of approximately 10 μ M against *E. coli* D22) (14). As a negative control fluorescein-labeled peptide, we used the same β -tubulin fragment as during the Western blotting, just without the addition of the spacer unit (27). The same heat shock proteins, controls, and LPS preparations were used as in the Western blotting, except DnaJ was not studied. The fluorescein-K-pyrrolicorin–DnaK binding study was repeated with three independent DnaK preparations: one purchased from Sigma, one from StressGen, and a third from Accurate. GroEL was acquired from Sigma and StressGen. The labeled peptides were used in fixed 1 nM concentrations. The initial concentration of the proteins was 4 μ M, and serial dilutions by two were done until the protein did not bind in at least two dilutions. The 4 μ M protein concentration is just barely below the lethal dose of the peptide and likely represents the raising stretch of the dose–response curve. The initial concentration of LPS was set to 0.5 mg/mL, and dilutions were made until 0.031 mg/mL. This concentration range roughly equaled that used for the heat shock proteins.

The N-terminally labeled pyrrolicorin peptide bound to DnaK with 50% higher millipolarization values over the

background (Figure 5). However, the N-terminally labeled pyrrolicorin peptide did not bind to Hsp70, GroES, GrpE nor to the negative control Ras (Figure 5 and Table 2). All these findings paralleled those with nitrocellulose membrane-bound proteins. In solution, the peptide bound to GroEL (with millipolarization values similar to DnaK) and less strongly to Hsp60. The interaction of pyrrolicorin with GroEL verified the sequencing data. The reason GroEL did not bind the peptide on Western-blot most likely lies in the nature of the interaction of GroEL with its ligands. GroEL consists of two heptameric rings of 57-kDa subunits that have a three-domain structure (28). The apical domain forms the opening of the cylinder and exposes a number of hydrophobic amino acid residues toward the center that are thought to interact with complementary surfaces of the polypeptide substrate. The intermediate segments allow a hinge-like opening and considerable twisting of the apical domains about the domain junctions (29). Mini-chaperones made of the polypeptide-binding fragments of GroEL assume the same folding pattern as in the full-size molecule (30), suggesting that the three-dimensional structure and the orientation of the hydrophobic amino acids are necessary for efficient ligand binding. Both the denaturing conditions during SDS–PAGE and the binding to the nitrocellulose membrane via the surface-exposed hydrophobic amino acids can easily eliminate the GroEL–ligand interaction. In this regard, it is significant that DnaK did not lose its ability to bind pyrrolicorin during Western blotting. This suggests that the binding of DnaK to pyrrolicorin is not dependent upon the global fold of the protein and that at least one peptide-binding site lies outside the conventional peptide-binding domain of DnaK. Alternatively, while in the case of the multimeric GroEL denaturation is inevitable, for some proteins, and maybe for DnaK, a partial restructuring can occur on the nitrocellulose membrane when exposed to certain buffers (31).

The LPS preparations bound to the N-terminally labeled pyrrolicorin peptide very strongly (Table 3). Little decrease in binding efficacy was detected at as low LPS concentration as 31 μ g/mL (calculating with a molecular weight of 20 kDa this corresponds to 1.5 μ M). The binding of DnaK or the two LPS preparations to pyrrolicorin appeared to be specific for the peptide sequence: neither the heat shock protein or the LPSs bound to the negative control fluorescein-labeled tubulin peptide (Table 3). In contrast, GroEL did bind to the tubulin sequence, with 50% over the background at 4 μ M protein concentration, a level comparable to pyrrolicorin binding. This suggests that GroEL recognized a generally unstructured peptide chain carrying a bulky hydrophobic appendage. Accordingly, GroEL does not seem to be the final bacterial protein target of the short, proline-rich insect antimicrobial peptides. Rather, it may play a role in the intermediate steps of the sequential molecular interaction cascade of the bacterial cell entry and killing by this peptide family (20).

Those biopolymers that showed strong binding to the N-terminally labeled pyrrolicorin (DnaK, GroEL, *E. coli* LPS, and *S. typhimurium* LPS) were tested for their binding to the C-terminally labeled pyrrolicorin peptide as well as to N-terminally labeled drosocin and apidaecin. The binding pattern to all three labeled peptides were very similar to that observed with the N-terminally labeled pyrrolicorin (Table 3). Apparently, both the C- and the N-termini of pyrrolicorin



No binding is observed to GroEL or DnaK at or below 0.5 μM concentration.

FIGURE 5: Fluorescence polarization with 5(6)carboxyfluorescein-K-pyrrocoricin and heat shock proteins.

Table 2: Competition Fluorescence Polarization with Heat Shock Proteins against Labeled and Unlabeled Pyrrocoricin^a

protein	millipolarization after preincubation with				
	pyrrocoricin		Conantokin G-Ala7		no peptide
	4 μM	8 μM	4 μM	8 μM	
GroEL	62	62	75	67	70 ± 10
DnaK	110	84	127	114	126 ± 5

^a In these experiments, 4 μM DnaK, GroEL, or Ras was premixed with 4 μM unlabeled pyrrocoricin, and after a 20-min incubation, the fluorescein-K-pyrrocoricin analogue was added in 1 nM concentration. The background reading (without any unlabeled peptide or protein) was 46 ± 7 millipolarization unit. In the presence of 4 μM Ras, this value was 52 ± 7 . As preincubation with 4 and 8 μM pyrrocoricin decreased the Ras readings with 16 and 27 millipolarization units, respectively, the readings for DnaK and GroEL were corrected with these values. The negative control peptide was Conantokin G-Ala7 (32), which is similar in size to pyrrocoricin (17 amino acid residues), but in contrast to the positively charged pyrrocoricin, which has a middle β -pleated sheet domain, is negatively charged, and is devoid of any extended structure (32). Accordingly, unlabeled pyrrocoricin could but Conantokin G-Ala7 could not compete for labeled pyrrocoricin binding.

orcin were involved in binding to DnaK, or the efficacy differences between the two termini could not be quantitated by fluorescence polarization.

The apparent differences in binding of pyrrocoricin to DnaK and GroEL suggested alterations in the binding mechanism or site of interaction. To examine this question in detail, we performed competition binding assays. During these studies, 4 μM DnaK, GroEL, or the negative control protein Ras was premixed with 4 or 8 μM unlabeled pyrrocoricin. After 20 min incubation time at room temperature, 1 nM N-terminally fluorescein-labeled pyrrocoricin was added, and the fluorescence anisotropy was recorded (Table 2). According to this assay, 4 μM unlabeled pyrrocoricin competed for GroEL binding, and an increase in the peptide did not further modify the binding to the unlabeled analogue. In contrast, the binding of the labeled peptide to DnaK decreased after preincubation with 4 μM pyrrocoricin, and it could be further decreased upon increasing the amount of the competing unlabeled analogue. Since we were still

far from the binding plateau, this may suggest that while GroEL has a single site for pyrrocoricin binding, the interaction with DnaK involves two independent fragments of the protein.

DISCUSSION

Apidaecin, drosocin, and pyrrocoricin share high degree of sequence homologies as well as similarities in the activity spectrum. It is reasonable to suppose that all three short proline-rich insect peptides kill bacteria by the same mode of action. Apidaecin was recently shown to enter the cells of Gram-negative bacteria through binding to a component of the outer membrane, followed by the interaction with a hypothetical transporter/receptor protein and finally to deactivate the bacteria via interaction with a third macromolecular target (20). The ribosome or perhaps other components of the protein synthesis machinery were suggested as potential candidates for being this last target biopolymer (20). In this study, we identified some of the players of this hypothetical cascade (Figure 6). According to our studies, the first step involves the interaction with bacterial LPS. In scenario A, the transporter proteins are heat shock/chaperonin proteins, i.e., GroEL and DnaK. The final target biopolymer may be the low molecular weight pyrrocoricin-binding band on the peptide blot. Positively charged peptides are known to interact with the negatively charged nucleic acids often in an unspecific manner (33) with the antibacterial peptide buforin II reportedly killing bacteria via binding to DNA and RNA and thus inhibiting cellular functions (34). Accordingly, the target macromolecule of the proline-rich antibacterial peptides can also be a nucleic acid. This scenario is similar to the one proposed by Castle and co-workers (20). Because our competition fluorescence polarization studies suggested a two-site interaction of pyrrocoricin with DnaK, we propose that the peptides bind to DnaK weakly inside the conventional peptide binding pocket as well as strongly outside. In this scenario B, DnaK and GroEL are the hypothetical transport proteins, and DnaK may also serve as the final target. The unidentified low molecular weight peptide-binding band is either a degradation product of DnaK

Table 3: Binding of Heat Shock Proteins and LPSs to Fluorescein-Labeled Peptides

protein or LPS	N-F-pyrrhocorin	C-F-pyrrhocorin	N-F-drosocin	N-F-apidaecin	N-F-tubulin
Ras	—	—	—	—	—
GroES	—	not tested	not tested	not tested	not tested
GrpE	—	not tested	not tested	not tested	not tested
GroEL	++ ^a	++	++	+	+
Hsp60	+	not tested	not tested	not tested	not tested
DnaK	++/++ ^b	++	++	++	—
Hsp70	—	not tested	not tested	not tested	not tested
<i>E. coli</i> LPS	++	+	++	++	—
<i>S. typhimurium</i> LPS	+++	+++	+++	+++	—

^a Studied with two GroEL preparations (Sigma and StressGen). N-F or C-F indicates the position of the fluorescein label (N- or C-terminus).
^b Studied with three different DnaK preparations (Sigma, Accurate, and StressGen).

Event	Castle et al. (20)	Our findings	
		Scenario A	Scenario B
Entry to cells	Binding to an outer membrane component	LPS	LPS
Invasion of periplasmic space	Receptor/docking molecule (transporter ?)	All hsp's	GroEL, DnaK Low MW band
Binding to target	Component of protein synthesis machinery (ribosome ?)	Low MW band Nucleic acid	DnaK

FIGURE 6: Hypothetical pathways of the bacterial cell entry of the short, proline-rich antibacterial peptides, and potential interacting protein candidates.

or is probably involved in the transport mechanism somewhere along the road from LPS to DnaK. This hypothesis is not inconsistent with the target protein being associated with protein synthesis (20). Members of the 70-kDa heat shock family proteins but not the 60-kDa chaperonins are known to interact with newly translated proteins both during translation and after their release from the ribosomes (35). It needs to be mentioned that the experimental details of competition fluorescence polarization are not fully developed, and these assays can result in surprising results (36) that are not supported by other fluorescence-based techniques (37).

The detection of functional differences between bacterial DnaK and the analogous human Hsp70 is not new to our studies. The IgG repertoire during intravesical bacille Calmette–Guerin immunotherapy in superficial bladder patients includes antibodies to GroEL and Hsp70 but not to DnaK (38). This finding emphasizes the significant structural and functional differences between mammalian Hsp70 and the corresponding bacterial DnaK and supports our findings and hypothesis that antibacterial peptides can inactivate DnaK without binding to Hsp70 and affecting its normal functions. According to the competition fluorescence polarization assay, DnaK may interact with pyrrhocorin at two independent sites. Because we were running these assays very close to the IC₅₀ of the labeled peptide, a single weak interaction site with Hsp70 probably remained undetected. For the identification of a possible pyrrhocorin-binding domain of DnaK outside the conventional peptide-binding pocket, we returned to the functional assay. We determined the antibacterial profile of a broad spectrum pyrrhocorin analogue (Table 4). According to this, the peptide killed *E. coli*, *Salmonella typhimurium*, *Micrococcus luteus*, *Bacillus megaterium*, and *Aerococcus viridans* but did not kill *Pseudomonas aeruginosa*, *Erwinia carotovora carotovora*, *Staphylococcus aureus*, and *Streptococcus pyogenes*. The pyrrhocorin analogues also kill *Agrobacterium tumefaciens* (14). The apparent lack of selectivity toward Gram-negative or Gram-positive

Table 4: In Vitro Antibacterial Activity of a Broad Spectrum Divalent Pyrrhocorin Analogue, Chex-Pyrrhocorin-2–19-Dap-[Chex-Pyrrhocorin-2–19-Dap(Ac)]

microorganism	IC ₅₀ in μM
Gram-Negative Bacteria	
<i>Escherichia coli</i> D22	0.1–1.2
<i>Salmonella typhimurium</i>	1.25–2.5
<i>Pseudomonas aeruginosa</i>	>40
<i>Erwinia carotovora carotovora</i>	>40
Gram-Positive Bacteria	
<i>Micrococcus luteus</i>	40–80 ^a
<i>Bacillus megaterium</i>	2.5–5
<i>Aerococcus viridans</i>	1.2–5
<i>Staphylococcus aureus</i>	>40
<i>Streptococcus pyogenes</i>	>40

^a The assay was performed in poor broth medium except for *M. luteus*, which was done in Luria-Bertani rich nutrient medium.

strains further confirms that the killing of bacteria is not related strongly to membrane binding. Rather, the specificity to certain bacterial strains may stem from altered binding to DnaK. In this case, at least one peptide-binding fragment should be sought in the variable domains of the protein. Careful comparison of various DnaK sequences (40) reveal high homology N-terminal to the peptide-binding region but considerably less homology downstream. In Figure 7, we aligned the DnaK sequences of some of the pyrrhocorin-responsive and nonresponsive bacterial strains as well as the sequence of the human analogue, Hsp70, starting from the conventional peptide-binding pocket (39) and extending to the carboxy termini. The structure of pyrrhocorin makes it prone to bind both inside and outside the conventional peptide-binding region. Based on screening of DnaK-bound peptide libraries (41), DnaK recognizes extended peptide strands within and positively charged residues outside the substrate binding cavity (42). In perfect harmony, pyrrhocorin displays a somewhat extended fragment in the middle of the sequence and positively charged residues all over, including the two biactive termini (14). Incidentally, two groups have reported peptide binding at the C-terminal area of DnaK. One of these identified the 518–545 residue stretch (43) (underlined in Figure 7) that serves as a lid over the peptide-binding pocket. According to the other, the highly negatively charged extreme C-terminal tetrapeptide of human Hsp70 (double underlined in Figure 7) binds a peptide substrate and affects ATPase activity (44). Yet another proof for C-terminal peptide binding comes from comparison of our peptide blot with Western blots developed with monoclonal antibodies directed against the C-terminal domain of mt Hsp70 (45). Antibody JG1, which is specific for the

ECOLI	VLLLDVTPLSLG I E TM GGVMT 408	
SALTY	VLLLDVTPLSLG I E TM GGVMT 408	
AGRTU	VLLLDVTPLSLG I E TL GGVFT 404	
BACME	VVLLDVTPLSLG I E TM GGVFT 379	
STRPY	VVLLDVTPLSLG I E TM GGVFT 379	
STAAU	VVLLDVTPLSLG I E IL GGRMN 379	
HUMAN	LLLLDVAPLSLG L E TA GGVMT 411	
ECOLI	TLIAKNTTIPTK HSQVFST AEDN Q SA V T I HVLQGERKRAADNKSLSGQFNLDGINPAPRGM 468	
SALTY	PLITKNTTIPTK HSQVFST AEDN Q SA V T I HVLQGERKRAADNKSLSGQFNLDGINPAPRGM 468	
AGRTU	RLIDRNTTIPTK KSQTFST AEDN Q SA V T I RVSQGEREMAQDNKLLGQFDLVGLPPSPRAV 464	
BACME	KLIERNTTIPTK KSQVFST AADS Q TA V D I HVLQGERPMSADNKTILGRFQLTDIPAPRGV 439	
STRPY	KLIDRNTTIPTK KSQVFST AADN Q PA V D I HVLQGERPMAADNKTILGRFQLTDIPAPRGI 439	
STAAU	TLIERNTTIPTK KSQIYST AVDN Q PS V D V HVLQGERPMAADNKTILGRFQLTDIPAPRGK 439	
HUMAN	ALIKRNTTIPTK QTQIFTT YSDN Q PG V L I QVYEGERAMTKDNLLGRFELSGIPAPRGV 471	
ECOLI	PQIEVTFDIDADGILHVSADKNSGKEQKITIKASSG-LNEDEIQKMVRDAEANAEDRK 527	hhhhhhhhhh hhhhhh
SALTY	PQIEVTFDIDADGILHVSADKNSGKEQKITIKASSG-LNEDEIQKMVRDAEANAEDRK 527	
AGRTU	PQIEVTFDIDANGIVQVSADKGTGKEQQIRIQASGG-LSDADIEKMVKDAEANAEDKK 523	
BACME	PQIEVSFDIDKNGIVNVRAKDLGTNKEQAITIKSSTG-LSDDIEDRMVKEAEENADADKQ 498	
STRPY	PQIEVTFDIDKNGIVNVRAKDLGTNKEQHIVIKSNDG-LSDEEIDRMVKDAEANAEDAK 498	
STAAU	PQIEVTFDIDKNGIVNVRAKDLGTNKEQRIITIQSSSS-LSDEEIDRMVKDAEVNAEDKK 498	
HUMAN	PQIEVTFDIDANGILNVATDKSTGKANKITITNDKGRLSKEEIERMVQAEKYKAEDDV 531	
ECOLI	FEELVQTRNQGDHLLHSTRKQVEEAGDK--LPADDKTAIESALTALETALKG---EDKAA 582	hhhhhhhhhh hhhhhh
SALTY	FEELVQTRNQGDHLLHSTRKQVEEAGDK--LPADDKTAIESALNALETALKG---EDKAA 582	
AGRTU	RRAGVEAKNQAESLIHSTKSVKEYGDK--VSETDRKAIEDAIASLKTAVEA---AEPDA 578	
BACME	RKEEVELRNEADQLVFTTEKTLKDLLEGK--VEEAETVKANEAKDALKAAIEK---NDLEE 553	
STRPY	RKEEVDLKNEDQAI FATEKTIKETEGK--GFDERDAQAQALDELKAAQES---GNLDD 553	
STAAU	RREEVDLRNEADSLVFQVEKTLTDLGEN--IGEDDKSAEEKKDALKTALEG---QDIED 553	
HUMAN	QREVSANNALESYAFNMKSAVEDEGLKGI SEADKKKVLKCKQEVISWLDANTLAEKDE 591	
ECOLI	IEAKMQELAQVSQKLMEIAQQQHAQQQTAGADASANNA----KDDDVVDAEFEEVKPKK--- 637	hhhhhhhh hhhhhh
SALTY	IEAKMQELAQVSQKLMEIAQQQHAQQQAGSADASANNA----KDDDVVDAEFEEVKDKK--- 637	
AGRTU	DDIQAKTQTLMEVSMKLGQAI IEAQQAEAGDASAE-----KDDVVADYEEIKDKKKA 633	
BACME	IKAKKDELQELVQALTVKLYEQAAQQAQAGE-----Q--GAQNDVVDAEFEEVNDKK-- 605	
STRPY	MKAKLEALNEKAQALAVKMYEQAAAAQQAQGAEGAQANDSANNDVVVDGEFTEK----- 608	
STAAU	IKSKKEELEKVIQELSAKVYEQAQQQQAQAG-----ANAGQNDSTVEDAEFNEVKDDKK-- 610	
HUMAN	FEHRRKELEQVCNPIISGLYQAGGPGPGGFGAQQP-----KGGSGSGPTIEEVD----- 641	

FIGURE 7: Alignment of various bacterial and human 70 kDa heat shock protein sequences in the C-terminal region. The residues in bold and bracketed indicate the peptide binding pocket according to ref 39. C-terminal DnaK sequences that bind peptides outside the conventional peptide-binding pocket are underlined. Singly underlined fragment is according to ref 43. Ref 44 identified the extreme C-terminus of human Hsp70 for peptide binding. The corresponding *E. coli* sequence is double underlined. The stretches of h letters above some domains indicate the predicted helical segments. The abbreviations of the bacteria are as follows: ECOLI: *Escherichia coli*; SALTY: *Salmonella typhimurium*; AGRTU: *Agrobacterium tumefaciens*; BACME: *Bacillus megaterium*; STRPY: *Streptococcus pyogenes*; STAAU: *Staphylococcus aureus*. According to the data presented in Figures 1 and 2, in our earlier paper (14), and in Table 4, the pyrrolicorin peptides kill bacteria containing ECOLI, SALTY, AGRTU, and BACME, while they do not affect species containing STRPY, STAAU, and HUMAN.

C-terminus of this 70-kDa heat shock protein, precipitates the full-length translated product as well as smaller products near 70 kDa and around 45 kDa (45). These smaller products are reported to result from alternative start sites for the initiation of translation and the lack of the N-terminus of this heat shock protein variant (46). In contrast, antibody JG3, which is specific for the N-terminus, recognizes only the full-length protein and none of the smaller fragments (45). As attractive as this explanation may seem, the proteinaceous nature of the small molecular weight band in our case was not supported by strong amidoblack staining. The identification of the exact DnaK binding site is currently in progress in our laboratories.

The design of new drugs can be based on either mimicking the conformation of known ligands or on the structure of the peptide-binding domain of the receptor. Here we provided a basis for both strategies. Earlier, we characterized the general fold of drosocin and pyrrolicorin, and we concluded that the antibacterial peptide ligands must assume two reverse turns at their terminal positions bridged by an extended peptide domain for full biological activity (14, 19). When the receptor's conformation is known, a candidate compound that has the necessary structural characteristics to permit its binding to the target protein sequence can be designed. Determination of the conformations of the pyrrolicorin-interacting fragments will be highly facilitated by the

availability of the high resolution structure of DnaK. The secondary structure and dynamics of the 10-kDa C-terminal variable domain (a likely binding site for peptides that are bacteria specific) was characterized by NMR and comprised of a rigid structure of four helices and the flexible C-terminal subdomain of 33 amino acids (47). A 21-kDa fragment just preceding this domain was studied by multinuclear, multi-dimensional NMR (48). This domain is observed to bind to its own C-terminus and offers a preview of the interaction of DnaK with other proteins and peptides.

The interaction of pyrrolicorin, drosocin, and apidaecin with the bacterial heat shock protein DnaK identifies DnaK as a convenient target for drug design. The current literature on heat shock/chaperone proteins is just too large to detail. Excellent reviews and monographs have been published in the past decade on the structure and function of these proteins (21–23). Significantly, DnaK is essential for bacterial growth at most temperatures (49). The C-terminal 10-kDa region appears to carry an important regulatory function (47), with many individual amino acid residues being involved in the various bioactivities of the protein (44). Currently, the heat shock 70 family of proteins are considered as suitable targets for drug development against inflammatory diseases and cancer. Hsp70, the human variant, rescues cells from apoptosis later in the death signaling pathway than any known anti-apoptotic protein, making it a tempting target

for antitumor therapeutic interventions (50). Cancer cells express high levels of heat shock proteins, so the modulation of Hsp70 expression was suggested to be a viable alternative in cancer therapy (51). The heat shock proteins appear to be good immunogens for both antibody and T-cell production (52). A subset of murine T-cells, produced upon delayed-type hypersensitivity to purified protein derivative, recognizes the heat shock proteins DnaK and GroEL (53). Likewise, OM-89, an anti-rheumatic bacterial extract, induces T-cell responses to heat shock proteins, Hsp60 and Hsp70, making it suitable for modulation of peripheral immunological tolerance in the treatment of rheumatoid arthritis (54). It is difficult to predict whether the antibacterial peptide–DnaK complexes will be disadvantageously immunogenic during therapeutic applications. Our positive *in vivo* data so far do not substantiate this concern.

Our current knowledge of the correlation of antibacterial action and heat shock proteins is very limited. It was observed that the interaction of *Salmonella typhimurium* and bactericidal/permeability increasing protein (BPI) results in the synthesis of a number of host–defense proteins, including HtpG (55). In solution, pyrrocoricin bound to GroEL and the human equivalent, Hsp60. This may explain why drosocin and unmodified pyrrocoricin, otherwise nontoxic peptides, became toxic to compromised animals (8, 14). Since the heat shock proteins appear to be expressed at a higher level upon bacterial infection, large doses of some of the Hsp60-binding antibacterial peptides may interfere with the natural defense mechanism of mammals. One of the referees mentioned that drosocin and pyrrocoricin are toxic to compromised animals, precisely the type of situation where a peptide antimicrobial drug might prove its value. It was also added that while the native peptides are toxic to infected animals with presumably high levels of heat shock proteins, the similarly high levels of heat shock proteins in bacteria may diminish activity of the peptides. A comparison of the *in vivo* and *in vitro* activities of pyrrocoricin and its Chex-pyrrocoricin-Dap(Ac) analogue may solve this controversy. The modified peptide exhibits a 10-fold decrease of the *in vitro* efficacy against *E. coli* D22, which probably reflects a decreased affinity to the target molecule. On the other hand, the modified peptide remains without toxicity in the entire 10–50 mg/kg peptide dose, even to compromised animals (14), in contrast to native pyrrocoricin. Apparently, the modified peptide retains some ability to bind to bacterial DnaK and kill bacteria, but the suboptimal binding to the mammalian heat shock protein(s) prevents the negative effects on the infection-combating efforts of the experimental animals. In conclusion, the antibacterial peptide drug leads need to be tested for their efficacy both *in vitro* and *in vivo* before any additional modification in their composition is initiated. Actually this recommendation coincides with our latest finding as to low *in vitro* activity of the antibacterial peptides does not necessarily indicate negligible *in vivo* efficacy (56).

The antibacterial actions of magainin 2, buforin II, and polylysine are all reduced against an *E. coli* variant that contains elevated levels of GroEL and DnaK (57), indicating a negative correlation between antimicrobial activity and interaction with heat shock proteins of the bacteria. However, these antimicrobial agents exhibit their actions either on the bacterial membrane or binding to DNA or RNA rather than

interacting with a housekeeping/regulatory protein (34, 58, 59). Nevertheless, all these peptides are strongly positively charged, just like drosocin, pyrrocoricin, and apidaecin. The referee suggested that unspecific binding of magainin 2, buforin II, or polylysine to DnaK or GroEL reduces their active concentration, requiring higher amounts for killing, and this may happen with the proline-rich family as well. Thus, pyrrocoricin-resistant microbial strains could actually bind DnaK better than *E. coli*. We tested this hypothesis by running peptide blots against *S. aureus* (resistant) and *M. luteus* (mildly responsive) lysates. Biotin-K-pyrrocoricin indeed labeled a band in the *S. aureus* lysate near the *E. coli* DnaK band. This would indicate that DnaK is not the target protein, only a carrier as depicted in the first column of Figure 6. However, such a DnaK band was absent in the blot using an *M. luteus* lysate. In addition, due to the near *E. coli* DnaK unspecific band combined with the different molecular weight of all DnaK proteins (Figure 7), quantitative conclusions are difficult to draw. Moreover, apparently the lack of *E. coli* DnaK binding of the inactive *all-D*-pyrrocoricin peptide suggests a positive correlation between killing and DnaK binding. Accordingly, it is not only the positive charge of the proline-rich peptide family that allows binding to DnaK. Rather, the true binding characteristics and perhaps therapeutic potency of these peptides lies in the actual sequences or in embedded motifs or conformations. The identification of the peptide-binding fragment of DnaK together with the determination of the conformation of the DnaK–peptide complexes will allow the design of strain-specific antimicrobial peptides.

ACKNOWLEDGMENT

The authors thank Drs. Hildegund C. J. Ertl, John D. Wade, Ian A. Smith, and Meryle Melnicoff for critical reading of the manuscript and valuable suggestions. The referees are also thanked for their suggestions and alternative explanations. The French-pressed *E. coli* lysate was kindly provided by Dr. Karl Johnson.

REFERENCES

1. Thomasz, A. (1994) *New Engl. J. Med.* 330, 1247–1251.
2. Bulet, P., Dimarcq, J.-L., Hetru, C., Lagueux, M., Charlet, M., Hegy, G., van Dorsselaer, A., and Hoffmann, J. A. (1993) *J. Biol. Chem.* 268, 14893–14897.
3. Cociancich, S., Dupont, A., Hegyi, G., Lanot, R., Holder, F., Hetru, C., Hoffmann, J. A., and Bulet, P. (1994) *Biochem. J.* 300, 567–575.
4. Casteels, P., Ampe, C., Jacobs, F., Vaeck, M., and Tempst, P. (1989) *EMBO J.* 8, 2387–2391.
5. Dimarcq, J.-L., Keppi, E., Dunbar, B., Lambert, J., Reichhart, J.-M., Hoffmann, D., Rankine, S. M., Fothergill, J. E., and Hoffmann, J. A. (1988) *Eur. J. Biochem.* 171, 17–22.
6. Mackintosh, J. A., Veal, D. A., Beattie, A. J., and Gooley, A. A. (1998) *J. Biol. Chem.* 273, 6139–6143.
7. Bulet, P., Urge, L., Ohresser, S., Hetru, C., and Otvos, L., Jr. (1996) *Eur. J. Biochem.* 238, 64–69.
8. Hoffmann, R., Bulet, P., Urge, L., and Otvos, L., Jr. (1999) *Biochim. Biophys. Acta* 1426, 459–467.
9. Andreu, D., and Rivas, L. (1998) *Biopolymers* 47, 415–433.
10. Ludtke, S., He, K., and Huang, H. (1995) *Biochemistry* 34, 16764–16769.
11. Steiner, H., Andreu, D., and Merrifield, R. B. (1988) *Biochim. Biophys. Acta* 939, 260–266.
12. Wimley, W. C., Selsted, M. E., and White, S. H. (1994) *Protein Sci.* 3, 1362–1373.

13. Cociancich, S., Ghazi, A., Hetru, C., Hoffmann, J. A., and Letellier, L. (1993) *J. Biol. Chem.* 268, 19239–19245.
14. Otvos, L., Jr., Bokonyi, K., Varga, I., Otvos, B. I., Hoffmann, R., Ertl, H. C. J., Wade, J. D., McManus, A. M., Craik, D. J., and Bulet, P. (2000) *Protein Sci.* 9, 742–749.
15. Casteels, P., and Tempst, P. (1994) *Biochem. Biophys. Res. Commun.* 199, 339–345.
16. Nishikata, M., Kanehira, T., Oh, H., Tani, H., Tazaki, M., and Kuboki, Y. (1991) *Biochem. Biophys. Res. Commun.* 174, 625–630.
17. Couto, M. A., Harwig, S. S., and Lehrer, R. I. (1993) *Infect. Immun.* 61, 2991–2994.
18. Basak, A., Ernst, B., Brewer, D., Seidah, N. G., Munzer, J. S., Lazure, C., and Lajoie, G. A. (1997) *Peptide Res.* 49, 596–603.
19. McManus, A., Otvos, L., Jr., Hoffmann, R., and Craik, D. J. (1999) *Biochemistry* 38, 705–714.
20. Castle, M., Nazarian, A., Yi, S. S., and Tempst, P. (1999) *J. Biol. Chem.* 274, 32555–32564.
21. Fink, A. L. (1999) *Physiol. Rev.* 79, 425–449.
22. Hendrick, J. P., and Hartl, F.-U. (1995) *FASEB J.* 9, 1559–1569.
23. Morimoto, R. I., Tissieres, A., and Georgopoulos, C., Eds. (1994) *Progress and Perspectives on the Biology of Heat Shock Proteins and Molecular Chaperones*, Cold Spring Harbor Laboratory, Cold Spring Harbor, NY.
24. Hoffmann, R., Dawson, N. F., Wade, J. D., and Otvos, L., Jr. (1997) *J. Peptide Res.* 50, 132–142.
25. Groisman, E. A. (1996) *Trends Microbiol.* 4, 127–128.
26. Inzana, T. J., and Apicella, M. A. (1999) *Electrophoresis* 20, 462–465.
27. Otvos, L., Jr., Pease, A. M., Wade, J. D., and Hoffmann, R. (1998) *Protein Pept. Lett.* 5, 207–213.
28. Braig, K., Otwinowski, Z., Hegde, R., Boisvert, D. C., Joachimiak, A., Horwich, A. L., and Sigler, P. B. (1994) *Nature* 371, 578–586.
29. Roseman, A. M., Chen, S., White, H., Braig, K., and Saibil, H. R. (1996) *Cell* 87, 241–251.
30. Buckle, A. M., Zahn, R., and Fersht, A. R. (1997) *Proc. Natl. Acad. Sci. U.S.A.* 94, 3571–3575.
31. Dunn, S. D. (1986) *Anal. Biochem.* 157, 144–153.
32. Zhou, L.-M., Szendrei, G. I., Fossom, L., Maccacchini, M.-L., Skolnick, P., and Otvos, L., Jr. (1996) *J. Neurochem.* 66, 620–628.
33. Hoffmann, R., Craik, D. J., Pierens, G., Bolger, R. E., and Otvos, L., Jr. (1998) *Biochemistry* 39, 13755–13764.
34. Park, C. B., Kim, H. S., and Kim, S. C. (1998) *Biochem. Biophys. Res. Commun.* 244, 253–257.
35. Braig, K. (1998) *Curr. Opin. Struct. Biol.* 8, 159–165.
36. Sakaguchi, K., Saito, S., Higashimoto, Y., Roy, S., Anderson, C. W., and Appella, E. (2000) *J. Biol. Chem.* 275, 9278–9283.
37. Kane, S. A., Fleener, C. A., Zhang, Y. S., Davis, L. J., Musselman, A. L., and Huang, P. S. (2000) *Anal. Biochem.* 278, 29–38.
38. Zlotta, A. R., Drowart, A., Huygen, K., De Bruyn, J., Shekarsarai, H., Decock, M., Pirson, M., Jurion, F., Palfliet, K., Denis, O., Mascart, F., Simon, J., Schulman, C. C., and Van Vooren, J. P. (1997) *Clin. Exp. Immunol.* 109, 157–165.
39. Zhou, X., Zhao, X., Burkholder, W. F., Gragerov, A., Ogata, C. M., Gottesman, M. E., and Hendrickson, W. A. (1996) *Science* 272, 1606–1614.
40. Karlin, S., and Brocchieri, L. (1998) *J. Mol. Evol.* 47, 565–577.
41. Rudiger, S., Germeroth, L., Schneider-Mergener, J., and Bukau, B. (1997) *EMBO J.* 16, 1501–1507.
42. Rudiger, S., Buchberger, A., and Bukau, B. (1997) *Nat. Struct. Biol.* 4, 342–349.
43. Zhang, J., and Walker, G. C. (1998) *Arch. Biochem. Biophys.* 356, 177–186.
44. Freeman, B. C., Myers, M. P., Schumacher, R., and Morimoto, R. I. (1995) *EMBO J.* 14, 2281–2292.
45. Green, J. M., Gu, L., Ifkovits, C., Kaumaya, P. T. P., Conrad, S., and Pierce, S. K. (1995) *Hybridoma* 14, 347–354.
46. Dominico, S. Z., DeNagel, D. C., Dahlseid, J. N., Green, J. M., and Pierce, S. K. (1993) *Mol. Cell. Biol.* 13, 3598–3610.
47. Bertelsen, E. B., Zhou, H., Lowry, D. F., Flynn, G. C., and Dahlquist, F. W. (1999) *Protein Sci.* 8, 343–354.
48. Wang, H., Kurochkin, A. V., Pang, Y., Hu, W., Flynn, G. C., and Zuiderweg, E. R. P. (1998) *Biochemistry* 37, 7929–7940.
49. Bukau, B., and Walker, G. C. (1990) *EMBO J.* 9, 4027–4036.
50. Jaattela, M., Wissing, D., Kokholm, K., Kallunki, T., and Egeblad, M. (1998) *EMBO J.* 17, 6124–6134.
51. Fuqua, S. A., Oesterreich, S., Hilsenbeck, S. G., Von Hoff, D. D., Eckardt, J., and Osborne, C. K. (1994) *Breast Cancer Res. Treat.* 32, 67–71.
52. Harada, M., Kimura, G., and Nomoto, K. (1998) *Biotherapy* 10, 229–235.
53. Pais, T. F., Silva, R. A., Smedegaard, B., Appelberg, R., and Anderson, P. (1998) *Immunology* 95, 69–75.
54. Bloemendal, A., Van der Zee, R., Rutten, V. P., van Kooten, P. J., Farine, J. C., and van Eden, W. (1997) *Clin. Exp. Immunol.* 110, 72–78.
55. Qi, S.-Y., Li, Y., Szyroki, A., Giles, I. G., Moir, A., and O'Connor, C. D. (1995) *Mol. Microbiol.* 17, 523–531.
56. Otvos, L., Jr. (2000) *J. Pept. Sci.* 6, 497–511.
57. Liang, J. F., and Kim, S. C. (1999) *J. Pept. Res.* 53, 518–522.
58. Matsuzaki, K., Murase, O., Fujii, N., and Miyajima, K. (1995) *Biochemistry* 34, 6521–6526.
59. Viljanen, P. (1987) *J. Antibiot.* 40, 882–886.

BI0012843